IEEE Access
Multidisciplinary | Rapid Review | Open Access Journal

Received October 28, 2021, accepted November 11, 2021, date of publication November 17, 2021,
date of current version November 29, 2021.

Digital Object Identifier 10.1109/ACCESS.2021.3128991

Estimation of Interpupillary Distance Based on Eye Movements in Virtual Reality Devices

JEONG-SIK KIM, BYEONG HUN AN, WON-BEEN JEONG, AND SEUNG-WOO LEE, (Senior Member, IEEE)
Department of Information Display, Kyung Hee University, Seoul 02447, South Korea

Corresponding author: Seung-Woo Lee (seungwoolee@khu.ac.kr)

This work was supported in part by the BK21 Fostering Outstanding Universities for Research (FOUR) funded by the Ministry of Education (MOE, South Korea).

This work involved human subjects or animals in its research. The authors confirm that all human/animal subject research procedures and protocols are exempt from review board approval.

ABSTRACT A mismatch between the interpupillary distance (IPD) and inter-optical system distance (IOSD) in virtual reality (VR) applications can lead to discomfort. The IOSD must be adjustable according to the user's IPD to solve this issue. In this study, we investigate IPD estimation methods by tracking eye movements such as conjugate eye movement (CEM) and vergence. We hypothesize that the distance between the two pupils maintained during the CEM and is identical to the IPD. The vergence-based method induces eye divergence and determines the IPD as the maximum distance between pupils. Experiments with visual stimuli to induce CEM and divergence were conducted. The average errors of the estimated IPDs for the CEM-based and vergence-based methods were 2.06 and 1.30 mm, respectively. Furthermore, the analysis results show that the proposed methods can effectively reduce the IPD-IOSD difference and are especially helpful for users with a small IPD. If the IOSD is adjusted to the IPD estimated by the proposed methods, then VR discomfort can be eliminated.

INDEX TERMS Eye movement, head-mounted display (HMD), interpupillary distance (IPD), IPD measurement, virtual reality (VR) device.

I. INTRODUCTION

Virtual reality (VR) is a computer-simulated environment separated from the real environment, which can provide a diverse experience that is impossible in the real world [1]–[3]. Most VR environments are mainly implemented with VR headsets, such as head-mounted display (HMD) devices. Generally, HMD devices comprise a pair of screens that display a different image to each eye. It provides a realistic virtual depth owing to the stereoscopic fusion of images.

Fig. 1 shows the major optical factors in the HMD device. Typically, an HMD device contains optical systems comprising a pair of screens and lenses. An inter-optical system distance (IOSD) is the horizontal interval between two optical systems. The optical systems should be fitted to the individual facial features, especially the interpupillary distance (IPD), to provide high-quality VR images. IPD is defined as the distance between the centers of the pupils when the optical axes of the eyes are parallel to each other [4], [5]. If there is a mismatch between IOSD and IPD, the user can suffer from troublesome symptoms during VR experiences, such

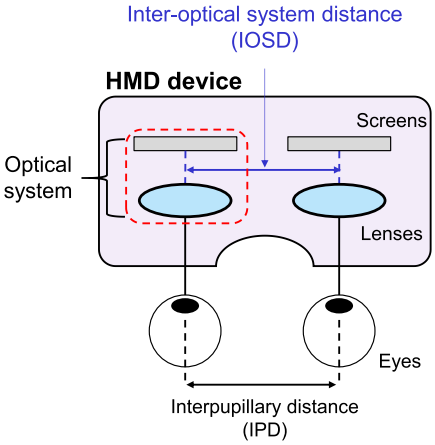

FIGURE 1. Concept of the interpupillary distance and the optical system in an HMD device.

The associate editor coordinating the review of this manuscript and approving it for publication was Liang-Bi Chen.

as eye fatigue, disorientation, and visual discomfort [6], [7]. Costello [8] found that misalignment contributes to prismatic distortion, which leads to eye strain and visual discomfort. Lewis and Griffin [9] showed that the discrepancy between IPD and IOSD can disrupt accommodation, convergence, and binocular fusion, causing eye strain. Mon-Williams *et al.* [10] also showed that the discrepancy induces an unstable binocular fusion, and it can be severe in children or adults who already have unstable binocular fusion. Because it results in the degradation of binocular fusion and visual acuity, the discrepancy may lead to strabismus and diplopia [10]. Furthermore, it can result in visual misperception in a VR environment [11], [12]. Utsumi *et al.* [11] investigated the effect of IPD mismatch on depth perception and found that it significantly misperceived the depth of a virtual object. Kim and Interrante studied the influence of a mismatch on perceiving an object's size in a virtual environment [12]. They found that an IOSD larger than IPD caused a significant decrease in perceived object size in VR. According to previous studies [13]–[15], females with smaller IPD than adult males tend to be more susceptible to these issues. This implies that people could have different VR experiences depending on their IPD, even if the same VR content is displayed. These uncomfortable feelings can lead to degradation of the quality of experience (QoE). Researchers have attempted to solve this issue in various aspects [16]–[19]. We performed a study focusing on the methods for matching the IPD and IOSD.

Whereas most VR headsets have been designed to have fixed screens and lenses, IPD varies depending on sex, age, race, and even individual [20]–[26]. We consider that the non-adjustable IOSD system is a key factor in these problems. Thus, we believe that an adjustable IOSD system is required for HMD devices. Most conventional HMD devices comprise fixed optical systems. Recently, however, several HMD devices that can ''manually'' adjust the distance between two lenses, such as Oculus Quest [27], HTC VIVE [28], and Sony PlayStation VR, are being released [29]. We believe that automatic adjustment of IOSD by estimating IPD in VR devices will be the next step. Therefore, an automatic IPD estimation is indispensable.

Several methods have been used to measure IPD [30]–[32]. Conventional methods, however, require a technician's help for accurate measurement or an extra cost to buy the device, such as a pupilometer [30]. Instead, Murray *et al.* [32] studied IPD measurements using an infrared (IR) camera. Eye locations were derived in 3D space by the camera, and the IPD was calculated as the difference between the two eye locations. This method cannot be applied in HMD because it requires a desktop environment and a viewing distance of 60 cm. PlayStation VR provides software for the self-measurement of IPD, but it also requires taking off the HMD and additional camera [29]. To overcome these issues, we have studied new methods to estimate IPD accurately using a VR headset with integrated IR cameras.

In this study, we introduce IPD measurement methods based on eye movements. Through the experiment, the accuracy and validity of each method were analyzed. We used IR cameras integrated into the VR headset, called an eye tracker. As various functions using an eye-tracking technique have been studied [18], [19], [33], [34], the eye tracker is becoming one of the major key features needed for future HMDs either to monitor the physical and mental states of the user or to provide more realistic virtual images [35]. We expect that this study will be one of the key functions of eye-tracking techniques.

II. EYE MOVEMENTS

A. CONJUGATE EYE MOVEMENT

Conjugate eye movement (CEM) is a movement of both eyes in the same direction to maintain a binocular gaze. It is used to either follow a moving object or change the direction of gaze without changing the depth of gaze. Based on this eye movement, we hypothesized the following: 1. Both eyes would rotate by the same angle in the same direction if the visual stimulus was presented to only one eye. 2. The distance between the two eyes would be maintained during CEM, as shown in Fig. 2(a), and the distance would be identical to that of IPD. Therefore, IPD can be estimated simply by measuring the distance between two eyes during CEM.

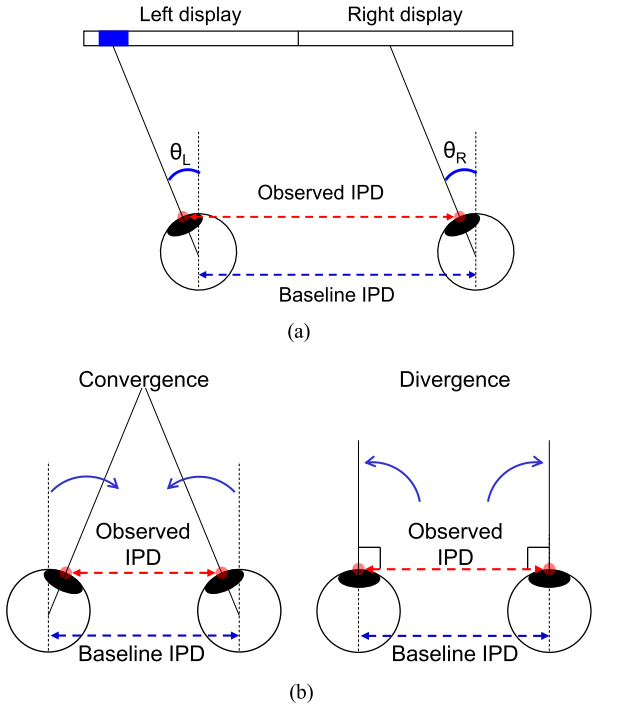

FIGURE 2. Two types of eye movements: (a) conjugate eye movement and (b) vergence.

B. EYE VERGENCE

The vergence is in contrast to the CEM. It is a simultaneous inward or outward movement of both eyes in opposite directions to maintain a single binocular vision. As shown in Fig. 2(b), there are two types of vergence: convergence,

which is the simultaneous inward movement of both eyes toward each other, and divergence, which is the simultaneous outward movement of both eyes away from each other. This method is based on the fact that the angle between the optical axis and a line connecting the eyeball front tops cannot be greater than 90° during divergence, as shown in Fig. 2(b). By tracking the interval between two pupil centers, the maximum value would be identical to that of the IPD.

III. EXPERIMENT

A. HARDWARE SETUP

A VR headset with integrated IR cameras was used, as shown in Fig. 3(a). The cameras recorded the eyes at a speed of 120 fps. To prevent a screen-door effect and distortion of a visual stimulus by the lens, we removed the lens and display parts in the headset. A pupilometer was used to measure the participants' true IPDs, as shown in Fig. 3 (b). A 24-inch LCD monitor whose screen was divided into two parts was used instead of the VR display, as shown in Fig. 3(c). The viewing distance was 30 cm. A chin rest was used to fix the participants' heads while wearing the VR headset.

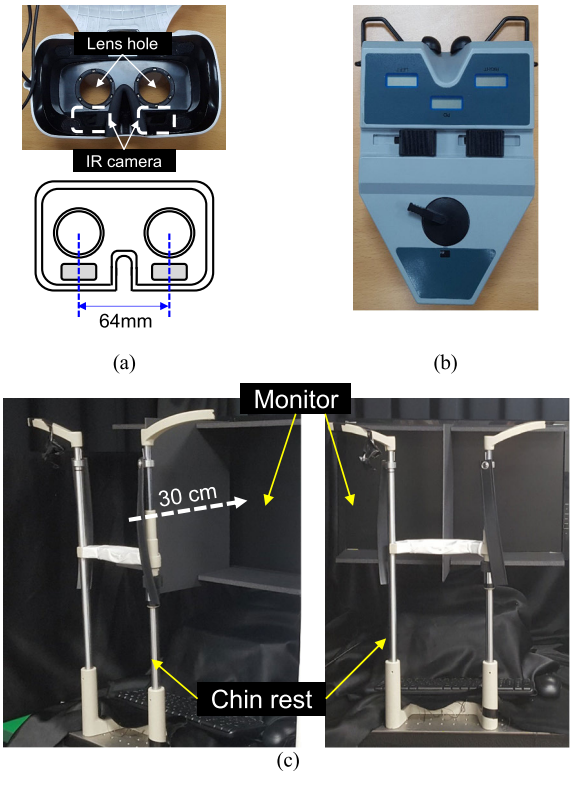

FIGURE 3. (a) Photograph (top) and schematic (bottom) of the VR headset with integrated IR cameras, (b) pupilometer, and (c) experimental setup.

B. VISUAL STIMULI

A white solid square with a viewing angle of 1° was used as the fixation point. Three types of visual stimuli, as shown in Fig. 4(a)–4(c), were used in the experiment: monocular stimulus (MS), binocular stimulus (BS), and no stimulus (NS). MS and BS conditions were used to induce conjugate eye movement and vergence, respectively. Participants can smoothly pursue a square moving horizontally at a certain speed. During the NS condition, no visual object was displayed on the screen. Table 1 describes the speed conditions for each stimulus type.

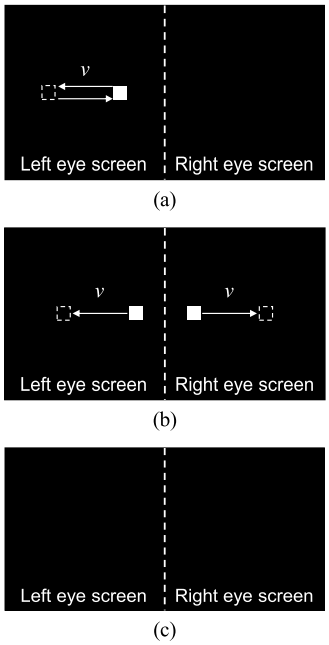

FIGURE 4. Three types of visual stimuli: (a) monocular stimulus, (b) binocular stimulus, and (c) no stimulus.

TABLE 1. Movement speeds under different stimulus conditions.

Stimulus type	Movement speed		
No stimulus	-		
Monocular stimulus	4°/s	8°/s	12°/s
Binocular stimulus	0.2°/s	0.4°/s	0.8°/s

C. PARTICIPANTS

Twenty-two observers (6 female, 16 male) participated in the experiment. Their average age was 25.8 years. We measured each participant's IPD using a pupilometer before the experiment. Fig. 5 shows the distribution of the true IPD of the participants. The number of participants was independent of the order of participation. The red and blue bars denote the results for the females and males, respectively. The detailed statistics are presented in Table 2. As with the previous researches, the IPD deviation according to individual and sex is observed.

D. PROCEDURE

We let the participant wear the VR headset and measured the distance between the eyes and the lens holes ($D_{eye-lens}$). $D_{eye-lens}$ was used to estimate the IPD in the proposed

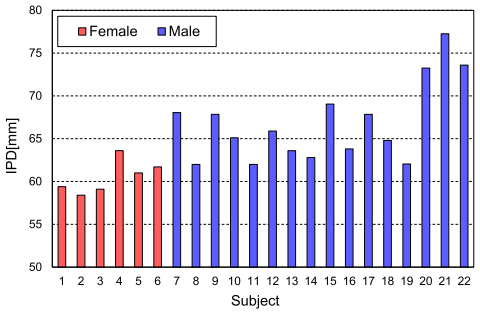

FIGURE 5. Measured IPDs of all participants by the pupilometer.

TABLE 2. Statistical results of measured IPDs.

		Female	Male	Total
IPD [mm]	Min.	58.4	62.0	58.4
	Mean	60.5	66.8	65.1
	Std.	1.8	4.5	4.8
	Max.	63.6	77.3	77.3

methods. Thereafter, the participants fixed their heads on the chinrest and checked whether the center of the monitor and the VR headset matched. The stimuli were presented in the order of MS, BS, and NS. The speed of the moving object was sequentially increased for each stimulus. The participants were requested to track the moving square with their eyes while fixing their heads. During the trial for the NS condition, the participants were allowed to move their gaze freely. A total of seven trials were performed, and the experiment was completed within ten minutes for each participant.

E. ESTIMATION OF IPD

The horizontal positions of each eye, depending on the time when the visual stimulus is presented, are shown in Fig. 6(a)–6(c). In the graph, the y-axis denotes the horizontal position of two pupils in the recorded images, and the unit is a pixel. The blue and red lines denote the horizontal positions of the right and left eyes, respectively. The solid black line denotes the interval between the two pupils. As shown in Fig. 6(a), both eyes move in the same direction as expected, and the interval is constantly maintained. In the CEM-based method, the MS and NS conditions were used, and the average value of the interval was estimated as IPD. Fig. 6(b) shows the interval at which the BS is presented. Because BS induces eye divergence, the interval increases over time, as shown in the inner graph in Fig. 6(b). In the vergence-based method, the maximum interval was estimated as the IPD.

The estimated IPD was calculated by summing the monocular pupillary distance (mono-PD) of each eye. Mono-PD was estimated using the following procedure: Before the estimation of mono-PD, preprocessing to correct perspective distortion was performed, as shown in Fig. 7(a). A perspective transform tool for Open CV-Python was used to correct perspective distortion. Because the IR camera aimed slightly upward, distortion was inevitable. The vertical axes of the image are parallelly aligned after perspective correction, and thus the horizontal interval is constant at any y-coordinate.

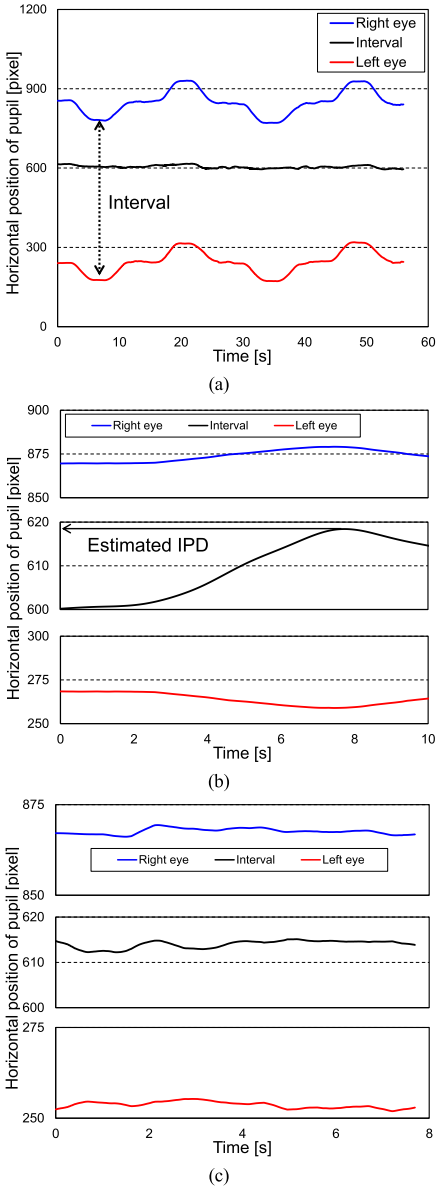

FIGURE 6. The horizontal positions of two pupils and their interval under (a) the monocular stimulus, (b) the binocular stimulus, and (c) the no stimulus conditions.

Thereafter, the mono-PDs were estimated from the corrected images. The horizontal resolution of the corrected images was 600 pixels. The center of the image corresponds to an actual distance of 32 mm from the center of the two IR cameras. As shown in Fig. 7(b), by converting the pixel interval to the actual distance, the mono-PD can be calculated using (1).

$$\begin{aligned} &\mathrm{PD_{Left}[mm]} \\ &\quad = 32[\mathrm{mm}] - \left\{(\mathrm{P_{x\_left}} - 300)[\mathrm{pixel}] \times U\left[{}^{\mathrm{mm}}/_{\mathrm{pixel}}\right]\right\} \\ &\mathrm{PD_{Right}[mm]} \\ &\quad = 32[\mathrm{mm}] + \left\{(\mathrm{P_{x\_right}} - 900)[\mathrm{pixel}] \times U\left[{}^{\mathrm{mm}}/_{\mathrm{pixel}}\right]\right\}, \end{aligned} \tag{1}$$

where P_{x_left} and P_{x_right} denote the x-coordinates of the left and right pupil positions, respectively. U is a conversion factor, which is a constant used to convert the unit of distance from the pixel in the image to mm, and it depends on $D_{eye-lens}$.

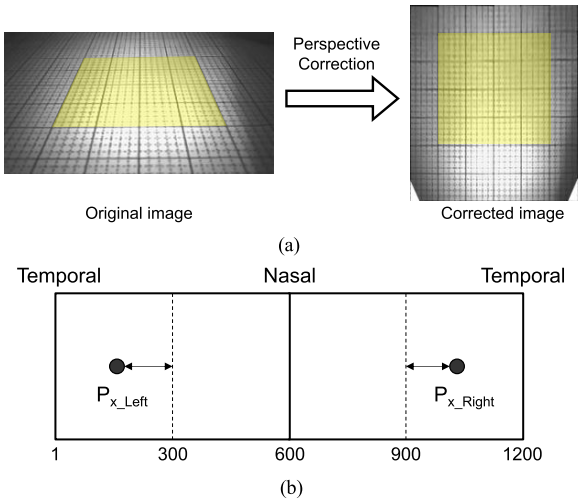

FIGURE 7. (a) Example images taken by the IR camera before and after perspective correction and (b) schematic of the images used in estimating mono-PD.

To determine the relationship between U and $D_{eye-lens}$, we took a picture of a sheet of graph paper and obtained the number of pixels per millimeter under various $D_{eye-lens}$ conditions, as shown on the left side of Fig. 7(a). Thereafter, we derived a linear model between U and $D_{eye-lens}$ through regression analysis using (2), whose coefficient of determination (R^2) was 0.99.

$$U = 0.0027 \times D_{eye\text{-}lens} - 0.0045 \tag{2}$$

IV. RESULTS

To investigate the accuracy of the proposed methods, IPDs estimated by the proposed methods (IPD_{est}) were compared to IPDs measured by the pupilometer (IPD_{meter}), which is considered to be the true IPD of the participant. The error was calculated by subtracting IPD_{est} from IPD_{meter} using (3).

$$IPD_{error} = IPD_{meter} - IPD_{est} \tag{3}$$

We obtained IPD errors for all conditions and performed a one-way analysis of variance. Fig. 8 shows the obtained data and multiple comparison results. In the chart, the small dots are the data for each participant, and the closed curves denote their frequency, that is, the density curve. The reddish, bluish, and grayish colored plots denote the results of the MS, BS, and NS conditions, respectively. Means and medians are described in each plot. Herein, they were computed using absolute error. In the MS condition, the errors were, on average, approximately 2 mm for all speed conditions. The medians for the errors were in the range of 1.89 mm and 2.16 mm. The distribution of IPD errors ranged from 0 mm to 4 mm, but the results over 4 mm were obtained under the conditions of 8°/s and 12°/s. The accuracy of the IPD estimation was the lowest under the NS condition. The average and median errors were 2.59 mm and 2.57 mm, respectively. Although the mean IPD_{error} for the NS condition was larger than the IPD_{error}s for the MS condition, no significant difference was observed between them. The IPD was estimated to have the highest accuracy under BS conditions. The average errors were 1.30, 1.33, and 1.53 mm for 0.2, 0.4, and 0.8°/s conditions, respectively. The errors under the BS condition were significantly lower than those under the NS condition. In addition, the error of 0.2°/s was significantly lower than that of all the MS conditions. Thus, even if it takes more time, the BS condition should be applied at a slower speed to obtain a more accurate IPD.

We investigated whether the IPD estimation methods can solve the IPD-IOSD mismatch problem in a VR environment. We compared the variance of the difference between the IPD and IOSD before and after adjusting for IOSD. Let us assume that $IOSD_{adj}$ is the IOSD adjusted to the estimated IPD. The IOSD of the VR headset used in this study was fixed at 64 mm ($IOSD_{64mm}$). Thus, the IPD-IOSD mismatch before adjustment becomes the difference between IPD_{meter} and 64 mm. After adjustment to IPD_{est}, the IPD-IOSD mismatch corresponds to the difference between IPD_{meter} and $IOSD_{adj}$. Fig. 9 shows the distributions of the IPD-IOSD mismatch before and after adjustment. In the graphs, the symbols and the black solid curve denote the IPD-IOSD difference values and their distribution curves, respectively. The mean values before and after adjustment were similar, but the SDs were significantly reduced. For some participants, the IOSD of the VR headset was approximately 5 mm larger or 13 mm smaller than their own IPDs before adjustment. The SD value was 4.8 mm. After adjustment, however, the IPD-IOSD mismatches were considerably reduced to 0.82–1.02 mm. Levene's test was performed to analyze the differences in the variance before and after adjustment. Table 3 describes the standard deviation and results of the Levene's test. The variances for the cases adjusted by the proposed methods with NS, MS, and BS were compared with the variance for the case before adjustment. We found that the proposed methods can significantly reduce the IPD-IOSD mismatch ($p < 0.05$), as shown in Table 3, once we can adjust the IOSD to IPD_{est} obtained by the proposed methods.

V. DISCUSSION

The CEM-based method was used in two stimuli conditions: MS and NS. The results of the IPD error for all participants were over 0 mm, which implies that the estimated IPD was smaller than the IPD measured by the pupilometer. We speculate that weak eye convergence is maintained during the CEM. Weak eye convergence was maintained even in the absence of a visual stimulus. This reveals that weak eye convergence might be natural, resulting in positive IPD_{error}s for all CEM conditions. We found that the error for the MS condition was smaller than that for the NS condition, which requires further investigation in our future work.

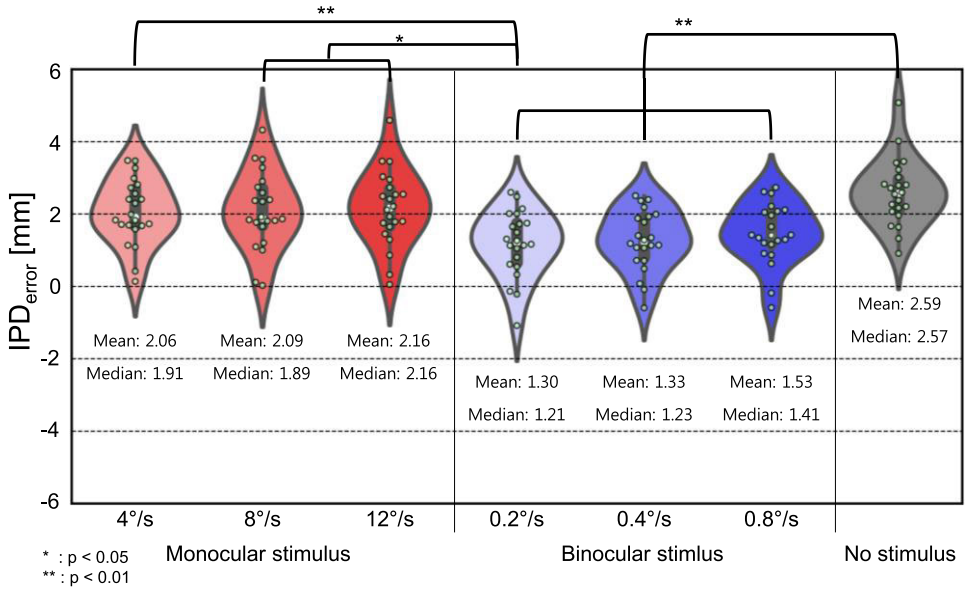

FIGURE 8. Distribution and the statistics of the IPD_{error}s for each condition.

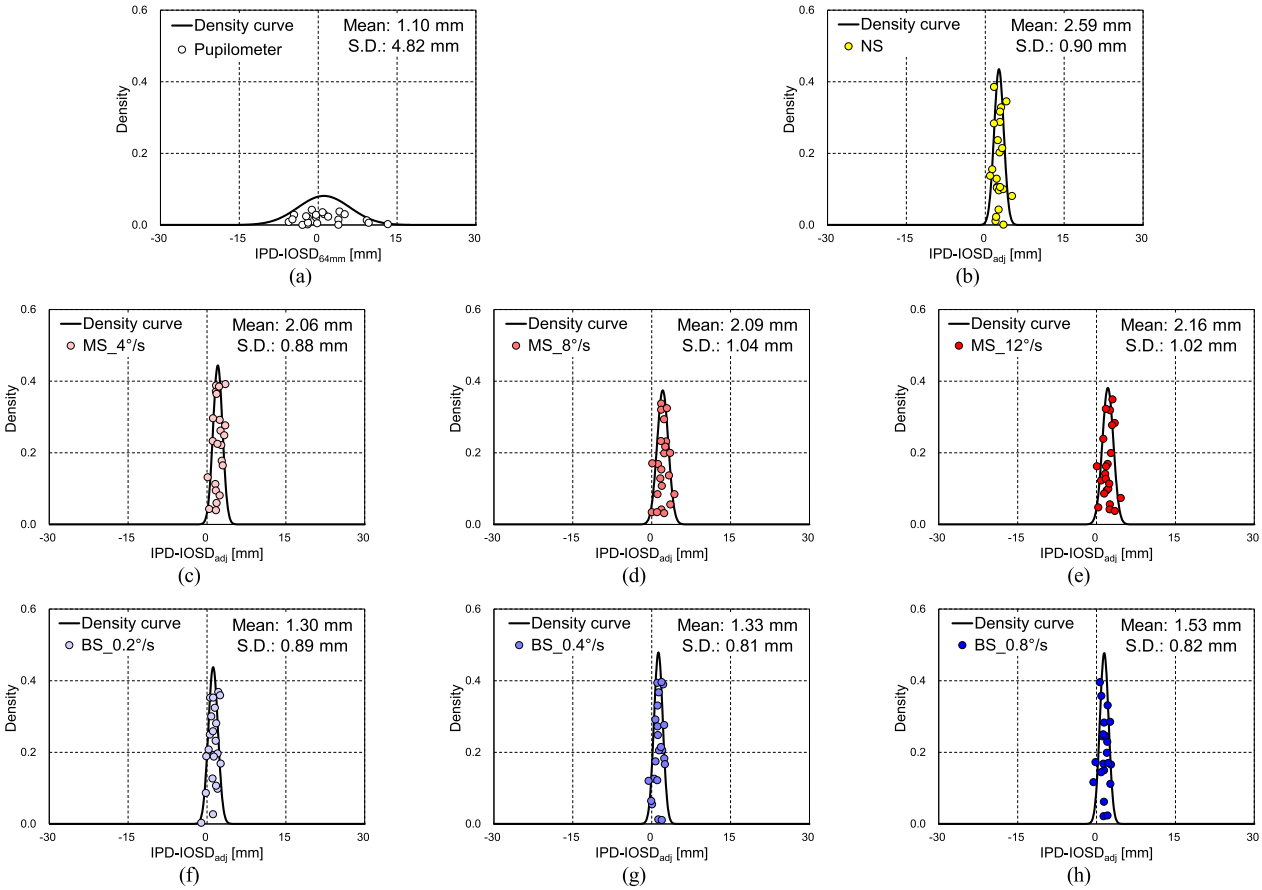

FIGURE 9. Distributions of IPD-IOSD differences: (a) between IPDs and IOSD with 64 mm, (b)-(h) between IPDs and the IOSD adjusted to the IPD_{est}s.

The vergence-based method induced eye divergence until the participant could not fuse the binocular images. Therefore, we can easily notice the IPD measurement condition in which the optical axes of the two eyes are parallel. Thus, it shows why a more accurate IPD can be obtained in the vergence-based method. However, contrary to the

TABLE 3. Results of Levene test.

Type			SD	Levene statistic			
				F	df1	df2	p
Before adjustment			4.82	-			
After adjustment	NS		0.90	23.48	1	42	0.00
	MS	4 °/s	0.88	23.10	1	42	0.00
		8 °/s	1.04	21.17	1	42	0.00
		12 °/s	1.02	21.58	1	42	0.00
	BS	0.2 °/s	0.89	23.36	1	42	0.00
		0.4 °/s	0.81	24.20	1	42	0.00
		0.8 °/s	0.82	24.44	1	42	0.00

CEM-based method, it is observed that a couple of results are negative, as shown in Fig. 9. This shows that, although it is less likely to occur, this method could induce excessive divergence for several users. Kim and Park [7] studied VR sickness depending on the mismatch between the IOSD and IPD. They reported that VR sickness critically increases when IOSD is 2 mm larger than the user's IPD, but it does not when the IOSD is 2 mm smaller than IPD. Thus, we consider that both proposed methods estimate the IPD within the allowable error range in terms of VR sickness. The CEM-based method has the advantage of being easy and fast and does not cause over-divergence, but it has a slightly larger error than the vergence-based method. Conversely, the vergence-based method can estimate IPD more accurately. The maximum eye divergence is induced until they are parallel; however, it may cause ocular fatigue or difficulty in binocular fusion depending on the person.

Although the VR device was used, the experiment was not performed in a VR environment. This is because we attempted to minimize the experimental variables, such as the uncontrollable screen-door effect and optical distortion. To create a visual stimulus in a VR environment, the optical characteristics of the lens must be considered owing to refraction and distortion. Thus, we removed the lens in the VR headset and used the monitor instead of the VR display. We verified that we could obtain IPD accurately by analyzing eye movements corresponding to visual stimuli with motion. Therefore, we anticipate that our proposed methods will work in a VR headset once visual stimuli accurately reflect optical distortion.

The goal of our study is to solve the IPD mismatch problem to improve the VR experience. Most VR headsets, including those used in this study, have lenses and displays designed for adult males. However, for some people with a small IPD, such as females, it might be too large to enjoy the VR content without visual discomfort [13]–[15]. According to previous studies, IOSD larger than IPD can lead to a surprising reduction in QoE for VR [7], [36]. To solve this problem, we focused on investigating IPD measurement methods using only a VR device as fundamental research for the auto-IOSD adjustment technique. We verified that the proposed methods could estimate the IPD accurately without an additional measuring apparatus. We believe that our work will contribute to reducing the negative symptoms caused by IPD mismatches. But there is a limitation that this secondary effect is based on literary inference. To verify this clearly, we will perform our study in a VR environment and evaluate its effectiveness in reducing visual discomfort when using VR devices in future work.

VI. CONCLUSION

In this study, we verified the proposed IPD measurement methods using an IR camera integrated into a VR headset. We investigated the IPD estimation methods based on eye movements. An experiment with three types of visual stimuli to induce two eye movements of the CEM and vergence was performed. The average IPD_{error}s of the CEM-based and vergence-based methods were 2.06 mm and 1.30 mm, respectively. This reveals that both methods can estimate the IPD with allowable accuracy. Furthermore, the analysis results showed that the proposed methods can effectively reduce the IPD-IOSD difference and are especially helpful for users with a small IPD.

Our findings suggest that the IR camera integrated in the VR headset can be used for measuring the IPD as well as for tracking gaze. We believe that this study shows the direction for VR headset technology to move forward. Many devices have been developed to be personalized, and they will be the same as VR devices. We believe that this study will be a foundation for a technique that automatically adjusts the alignment between IOSD and IPD, and this technique would be a key to solving the problems caused by IPD-IOSD mismatch. Even now, there are people who struggle to play VR content owing to a small IPD. It is expected that this study will help these people enjoy VR content without any discomfort. Therefore, we believe that this study will contribute to enhancing the VR experience and increasing the user base for VR.

ACKNOWLEDGMENT

The authors would like to thank the LooxidLabs for supporting the head-mounted display device (LooxidVR) and the analysis software for this study.

REFERENCES

[1] S. Mandal, "Brief introduction of virtual reality & its challenges," *Int. J. Eng. Res.*, vol. 4, no. 4, pp. 304–309, Apr. 2013.
[2] P. Cipresso, I. A. C. Giglioli, M. A. Raya, and G. Riva, "The past, present, and future of virtual and augmented reality research: A network and cluster analysis of the literature," *Frontiers Psychol.*, vol. 9, pp. 1–20, Nov. 2018.
[3] P. Scarfe and A. Glennerster, "The science behind virtual reality displays," *Annu. Rev. Vis. Sci.*, vol. 5, no. 1, pp. 529–547, Sep. 2019.
[4] B. J. Holland and J. Siderov, "Repeatability of measurements of interpupillary distance," *Ophthalmic Physiol. Opt.*, vol. 19, no. 1, pp. 74–78, Jan. 1999.
[5] R. L. Barretto and R. H. Mathog, "Orbital measurement in black and white populations," *Laryngoscope*, vol. 109, no. 7, pp. 1051–1054, Jul. 1999.
[6] J. J. LaViola, Jr., "A discussion of cybersickness in virtual environments," *ACM SIGCHI Bull.*, vol. 32, no. 1, pp. 47–56, 2000.
[7] H. Kim and J. H. Park, "Effects of simulator sickness and emotional responses when inter-pupillary distance misalignment occurs," in *Proc. Int. Conf.*, Ihsi, CA, USA, Feb. 2019, pp. 442–447.

[8] P. J. Costello, "Health and safety issues associated with virtual reality: A review of current literature," in *Proc. Conf. Tech. Rep. Ser.*, Loughborough, U.K., 1997, pp. 371–375.
[9] C. H. Lewis and M. J. Griffin, "Human factors consideration in clinical applications of virtual reality," in *Proc. Virtual Reality Neuro-Psycho-Physiol.*, Amsterdam, The Netherland, 1997, pp. 35–56.
[10] M. Mon-Williams, J. P. Warm, and S. Rushton, "Binocular vision in a virtual world: Visual deficits following the wearing of a head-mounted display," *Ophthalmic Physiol. Opt.*, vol. 13, no. 4, pp. 387–391, Oct. 1993.
[11] A. Utsumi, P. Milgram, H. Takemura, and F. Kishino, "Investigation of errors in perception of stereoscopically presented virtual object locations in real display space," in *Proc. Hum. Factors Ergon. Soc. Annu. Conf.*, Los Angeles, CA, USA, Oct. 1994, pp. 250–254.
[12] J. Kim and V. Interrante, "Dwarf or giant: The influence of interpupillary distance and eye height on size perception in virtual environments," in *Proc. ICAT EGVE*, Adelaide, NSW, Australia, Nov. 2017, pp. 22–24.
[13] K. Stanney, C. Fidopiastis, and L. Foster, "Virtual reality is sexist: But it does not have to be," *Frontiers Robot. AI*, vol. 7, pp. 1–19, Jan. 2020.
[14] J. Munafo, M. Diedrick, and T. A. Stoffregen, "The virtual reality head-mounted display oculus rift induces motion sickness and is sexist in its effects," *Exp. Brain Res.*, vol. 235, no. 3, pp. 889–901, Dec. 2016.
[15] K. M. Stanney, K. Kingdon, I. Nahmens, and R. S. Kennedy, "What to expect from immersive virtual environment exposure: Influences of gender, body mass index, and past experience," *Hum. Factors*, vol. 45, no. 3, pp. 504–522. Aug. 2003.
[16] H. Duan, G. Zhai, X. Min, Y. Zhu, Y. Fang, and X. Yang, "Perceptual quality assessment of omnidirectional images," in *Proc. IEEE Int. Symp. Circuits Syst. (ISCAS)*, Florence, Italy, May 2018, pp. 1–5.
[17] W. Sun, X. Min, G. Zhai, K. Gu, H. Duan, and S. Ma, "MC360IQA: A multi-channel CNN for blind 360-degree image quality assessment," *IEEE J. Sel. Topics Signal Process.*, vol. 14, no. 1, pp. 64–77, Jan. 2020.
[18] B. Guenter, M. Finch, S. Drucker, D. Tan, and J. Snyder, "Foveated 3D graphics," *ACM Trans. Graph.*, vol. 31, no. 6, pp. 1–10, Nov. 2012.
[19] A. Patney, J. Kim, M. Salvi, A. Kaplanyan, C. Wyman, N. Benty, A. Lefohn, and D. Luebke, "Perceptually-based foveated virtual reality," in *Proc. ACM SIGGRAPH Emerg. Technol.*, Anaheim, CA, USA, Jul. 2016, pp. 1–2.
[20] N. A. Dodgson, "Variation and extrema of human interpupillary distance," in *Proc. Stereoscopic Displays Virtual Reality Syst.*, Surfing, CA, USA, 2004, pp. 36–46.
[21] E. P. Osuobeni and K. A. Al-Musa, "Gender differences in interpupillary distance among arabs," *Optometry Vis. Sci.*, vol. 70, no. 12, pp. 1027–1030, Dec. 1993.
[22] C. MacLachlan and H. C. Howland, "Normal values and standard deviations for pupil diameter and interpupillary distance in subjects aged 1 month to 19 years," *Ophthalmic Physiol. Opt.*, vol. 22, no. 3, pp. 175–182, May 2002.
[23] J. S. Pointer, "The interpupillary distance in adult Caucasian subjects, with reference to 'readymade' reading spectacle centration," *Ophthalmic Physiol. Opt.*, vol. 32, no. 4, pp. 324–331, Jul. 2012.
[24] Y. Yildirim, I. Sahbaz, T. Kar, G. Kagan, M. T. Taner, I. Armagan, and B. Cakici, "The Evaluation of interpupillary distance in the Turkish population," *Clin. Ophthalmol.*, vol. 9, pp. 1413–1416, Aug. 2015.
[25] H. Fesharaki, L. Rezaei, F. Farrahi, T. Banihashem, and A. Jahanbkhshi, "Normal interpupillary distance values in an Iranian population," *J. Ophthalmic Vis. Res.*, vol. 7, no. 3, pp. 231–234, Jul. 2012.
[26] T. Filipovic, "Changes in the interpupillary distance (IPD) with ages and its effect on the near convergence/distance (NC/D) ratio," *Coll. Antropol.*, vol. 27, no. 2, pp. 723–727, Mar. 2003.
[27] *Facebook Technologies*. Accessed: Jul. 13, 2021. [Online]. Available: https://www.oculus.com
[28] *HTC*. Accessed: Jul. 13, 2021. [Online]. Available: https://www.vive.com/us
[29] *Sony Interactive Entertainment*. Accessed: Jul. 13, 2021. [Online]. Available: https://www.vive.com/us
[30] T. T. Mcmahon, E. L. Irving, and C. Lee, "Accuracy and repeatability of self-measurement of interpupillary distance," *Optometry Vis. Sci.*, vol. 89, no. 6, pp. 901–907, Jun. 2012.
[31] M. Y. Mommaerts and B. A. M. M. L. Moerenhout, "Reliability of clinical measurements used in the determination of facial indices," *J. Cranio-Maxillofacial Surg.*, vol. 36, no. 5, pp. 279–284, Jul. 2008.
[32] N. P. Murray, M. Hunfalvay, and T. Bolte, "The reliability, validity, and normative data of interpupillary distance and pupil diameter using eye-tracking technology," *Transl. Vis. Sci. Technol.*, vol. 6, no. 4, pp. 1–12, Jul. 2017.
[33] Y. Wang, G. Zhai, S. Zhou, S. Chen, X. Min, Z. Gao, and M. Hu, "Eye fatigue assessment using unobtrusive eye tracker," *IEEE Access*, vol. 6, pp. 55948–55962, 2018.
[34] Y. Wang, G. Zhai, S. Chen, X. Min, Z. Gao, and X. Song, "Assessment of eye fatigue caused by head-mounted displays using eye-tracking," *Biomed. Eng. OnLine*, vol. 18, no. 1, pp. 1–19, Nov. 2019.
[35] C. Mai and T. Steinbrecher, "Evaluation of visual discomfort factors in the context of HMD usage," in *Proc. IFIP Conf. Hum. Comput. Interact.*, Mumbai, India, Sep. 2017, pp. 1–4.
[36] E. Chang, H. T. Kim, and B. Yoo, "Virtual reality sickness: A review of causes and measurements," *Int. J. Hum.-Comput. Interact.*, vol. 36, no. 17, pp. 1658–1682, Jul. 2020.

JEONG-SIK KIM received the B.S. and M.S. degrees in information display from Kyung Hee University, Seoul, South Korea, in 2016 and 2018, respectively, where he is currently pursuing the Ph.D. degree with the Department of Information Display. He has been involved in driving technology for visibility, color, and motion performance of the displays.

BYEONG HUN AN received the B.S. degree from Kyung Hee University, Seoul, South Korea, in 2019, where he is currently pursuing the M.S. degree with the Department of Information Display. His current research interests include computer vision and sensing methodologies of touch screen panel.

WON-BEEN JEONG received the B.S. degree in information display from Kyung Hee University, Seoul, South Korea, in 2019, where he is currently pursuing the master's degree with the Department of Information Display. His research interests include visual perception and driving technology for low-power display.

SEUNG-WOO LEE (Senior Member, IEEE) received the B.S. and M.S. degrees in electrical engineering and the Ph.D. degree from the Korea Advanced Institute of Science and Technology, in 1993, 1995, and 2000, respectively, where he conducted research on integrated driver circuits for poly-Si TFT-LCDs. He joined Samsung, in 2000, where his work has focused on the development of key driving technologies for active-matrix liquid-crystal displays. He has played a key role in image quality enhancement, high-end LCD timing-controller design, FPGA evaluation of new driving schemes, next-generation LCD interface technologies, and advanced LCD driving schemes for large-size TV applications. He was also in charge of the development of analog-digital mixed-signal ICs for TFT-LCDs. He joined Kyung Hee University, Seoul, South Korea, where he has been studying novel display systems and visual perception and is currently a Full Professor with the Department of Information Display. He has been active as a Senior Member of Society for Information Display, since 2010. He was a recipient of the 2008 Chester Sall Award from IEEE Consumer Electronics Society, in 2010.